LAWRENCE
LIVERMORE
NATIONAL
LABORATORY

LLNL-CONF-413208

Progress in Initiator Modeling

C. A. Hrousis, J. S. Christensen

May 21, 2009

40th International Annual Conference of ICT
Karlsruhe, Germany
June 23, 2009 through June 26, 2009

Disclaimer

PROGRESS IN INITIATOR MODELING

Constantine A. Hrousis, John S. Christensen

Lawrence Livermore National Laboratory
7000 East Avenue, Livermore, California 94550 USA

(925) 423-4744
hrousis1@llnl.gov

Abstract

There is great interest in applying magnetohydrodynamic (MHD) simulation techniques to the designs of electrical high explosive (HE) initiators, for the purpose of better understanding a design's sensitivities, optimizing its performance, and/or predicting its useful lifetime. Two MHD-capable LLNL codes, CALE and ALE3D, are being used to simulate the process of ohmic heating, vaporization, and plasma formation in the bridge of an initiator, be it an exploding bridgewire (EBW), exploding bridgefoil (EBF) or slapper type initiator. The initiation of the HE is simulated using Tarver Ignition & Growth reactive flow models. 1-D, 2-D and 3-D models have been constructed and studied. The models provide some intuitive explanation of the initiation process and are useful for evaluating the potential impact of identified aging mechanisms (such as the growth of intermetallic compounds or powder sintering). The end product of this work is a simulation capability for evaluating margin in proposed, modified or aged initiation system designs.

Introduction

This work builds upon previously reported work in modeling the performance of new and aged EBWs.[1] Present models of EBW detonators include Ignition and Growth (I&G) Reactive Flow Models for the initiating explosive (most commonly PETN),[2] and the response of the explosive is dynamically coupled with the excitation from the EBW.

Most of our early work has been in the exploration of simple one- and two-dimensional models of EBWs with PETN using the two-dimensional LLNL-developed hydrodynamic code CALE. Simple 1-D models, in particular, lend some basic insight into how EBW detonators function – how electrical energy is converted to heat, changing the phase of the EBW so quickly that it explodes and sends shocks into the surrounding medium (PETN). Some of these basic insights are discussed here, and more complicated models of other geometries (such as EBFs and slappers) are introduced as our current and future work.

EBW Modeling Methods & Results

Figure 1 shows basic output from a typical 1-D CALE model of a gold EBW surrounded by half-dense PETN. A convenient method for displaying such results is the "streak plot" where the variable of interest (density, pressure, etc.) is plotted as a function of space (radius, in the y-direction) and time (in the x-direction). This shows the geometry of the EBW-PETN system at all times, as well as the variable of interest at all locations in the model. Though the 1-D models are simplified, they lend insight into the dynamics of EBW detonator function. In general, the EBWs in these models experience four "phases" that appear distinct in these simple models though are more blurred in real detonator function. The first of these phases is the "heating phase" (occurring for this geometry up through 540 ns), during which the current density builds, causing ohmic heating of the EBW. The resistance grows slowly until the EBW melts, causing the resistance to grow more rapidly until the vaporization temperature is reached. At this temperature, the "vapor expansion phase" (540-720 ns) begins, as the gold vaporizes and begins seeking a lower density, sending a relatively weak shock into the surrounding PETN. In these simple models, the latent heat of vaporization is neglected, thus vaporization is instantaneous (an obvious discrepancy with experimental observations), but the result of vastly increased EBW resistance and a spike in bridge voltage ("burst") is captured. The vapor expansion phase is marked by decelerating expansion of the gold gas with density moving to the wire exterior, still heating as the plasma formation temperature is approached. At this point, the "plasma expansion phase" (720-940 ns) begins, and the

EBW exhibits an accelerating runaway expansion as the EBW grows to large diameters as a thin tube of gold plasma that is continually decreasing in density as the circuit current builds to its maximum. It is during this phase that the EBW sends its largest, fastest shocks into the PETN. The peak circuit current marks the beginning of the final "collapse / recovery phase" (beyond 940 ns) as the current decays (recovers) and the plasma collapses inward due to forces induced by the existing magnetic field. These basic phases of EBW dynamics appear in all our typical EBW simulations.

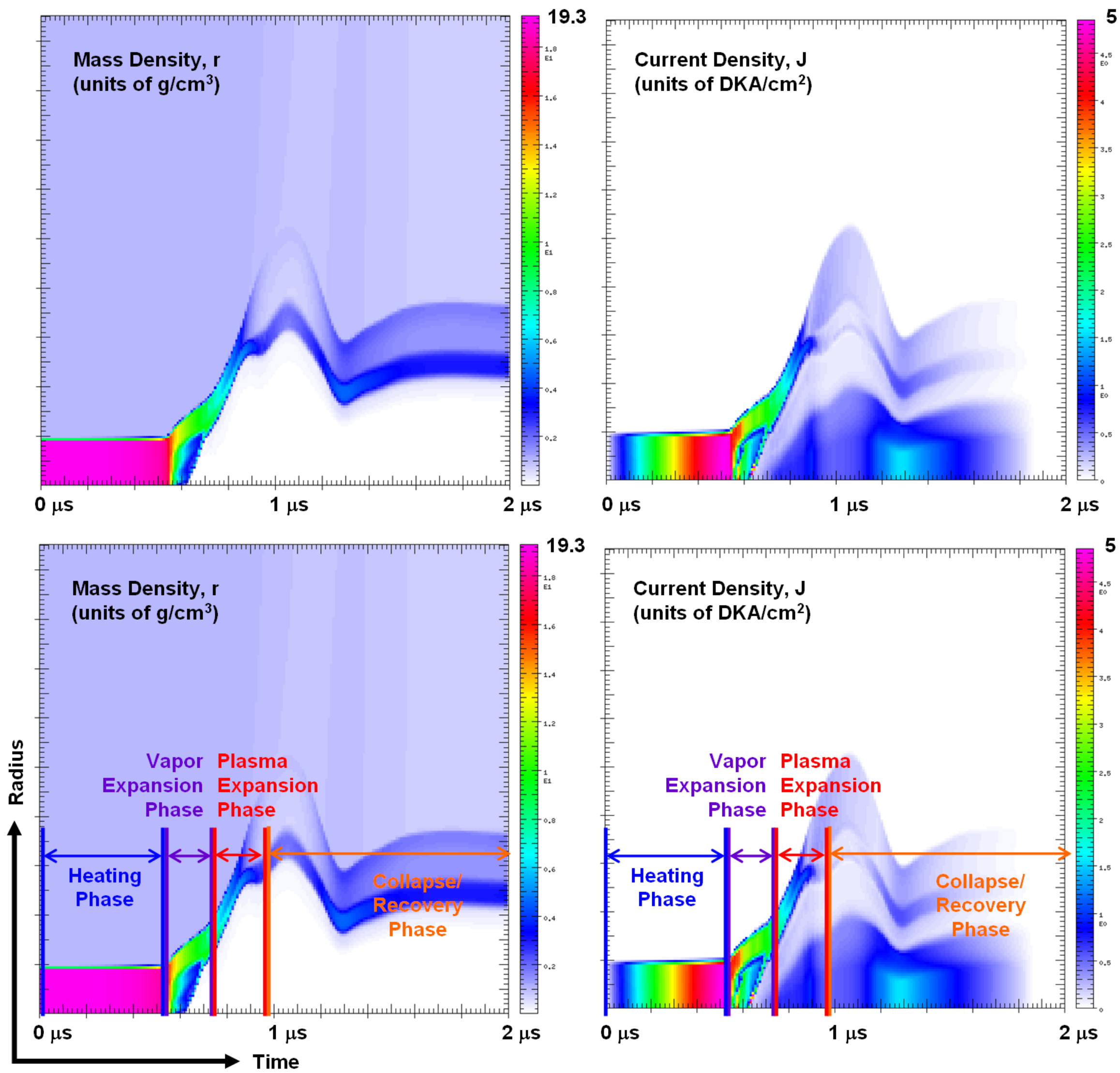

Figure 1. Streak plots showing basic one-dimensional EBW dynamic trends. Left panels show density plotted as a function of radius and time; right panels show current density. Bottom panels include labels for qualitative EBW dynamic "phases" (discussed in text).

Figure 2 demonstrates a qualitative comparison between electrical waveforms as observed in experiment, and as simulated by CALE in these 1-D models. The biggest discrepancy is the neglect of the latent heat of vaporization, and the early spike in voltage that produces. Also, because less energy is drained from the circuit during vaporization, a larger current peak results. Though not shown here (for brevity), experimental streak images of exploding wires show the same weak vaporization shock, followed by strong plasma-formation shocks as are seen in these simulations. The fact that multiple shock waves of increasing strength and speed are emitted from the EBW is important in understanding how the surrounding powder is initiated.

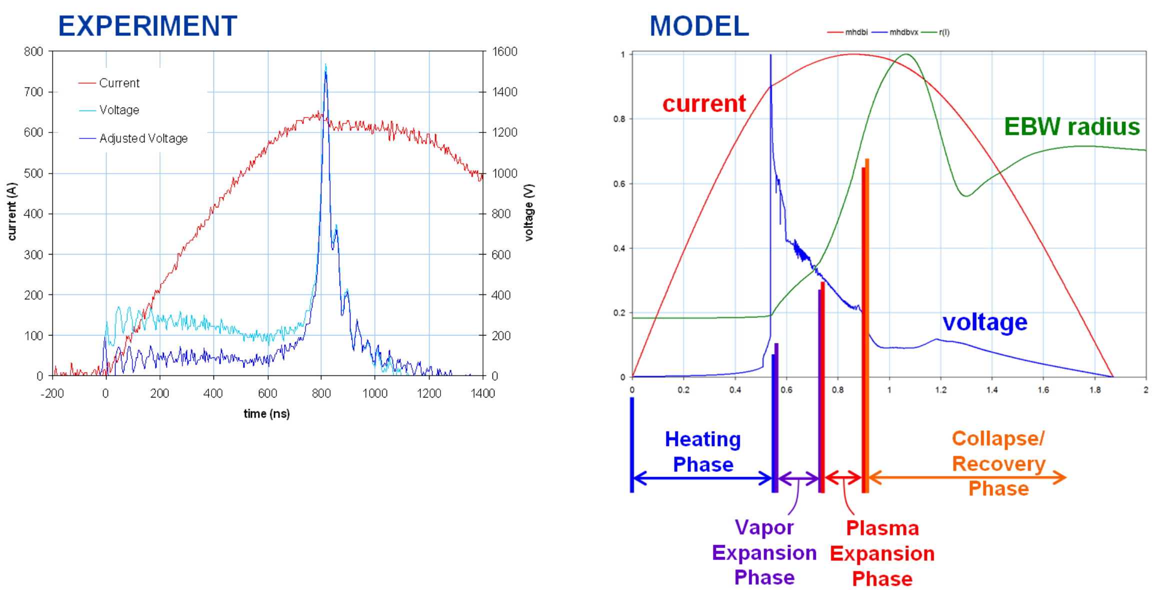

Figure 2. Qualitative comparison of experimental results with 1-D model. "Phases" are divided by electrical or hydrodynamic events, which appear instantaneous in models, but in reality are smeared over time and not so distinct. The measured voltage is "adjusted" to remove induced voltage effects, allowing a more direct comparison. Wiggles or jitter in the experimental waveforms are not only due to diagnostic uncertainties, but to transmission line effects, which are not simulated.

The dynamics of the EBW is largely unaffected by the surrounding powder because the time scale of the EBW dynamics is significantly shorter than the powder reaction. The powder, however, is entirely driven by the shocks sent into it by the EBW. **Figure 3** shows more streak-plot simulation results, but at the scale of the powder (much larger than the EBW). Most noteworthy is the fact that near the EBW, the powder initiates very slowly, taking about half a microsecond to completely initiate, and the further away from the EBW, the faster initiation occurs. This is because the earlier shocks are weaker and slower, and are swept up by and combine with the later, stronger shocks. The net result is a stronger, faster initiation, away from the bridge, after the contributing shocks have coalesced. This is further enhanced by contributing pressures from partial reactions of the powder. The powder initiation completes away from the bridge first, and to some extent burns backward toward the EBW. This build-up of initiation is in qualitative agreement with LLNL experiments on "cut-back" detonators (not shown here, for brevity).

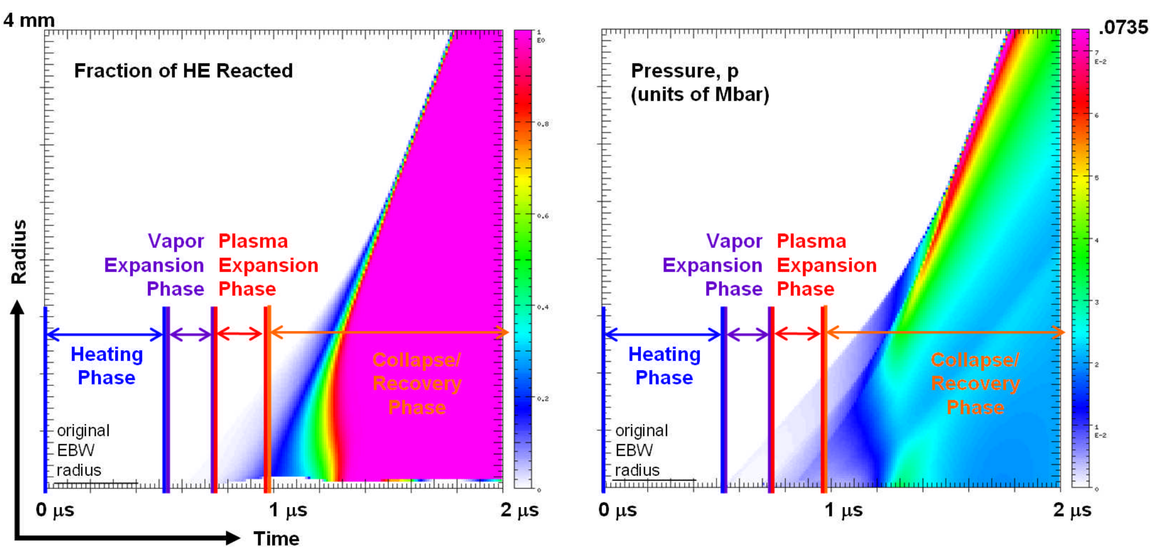

Figure 3. 1-D model results of powder response to EBW burst. Note that the vertical (distance) scale is much larger than in **Figure 1**, and that the EBW itself occupies only a small volume at small radii. The left panel shows fraction of HE reacted, and that near the EBW the reaction is slow, occurring more quickly some distance away from the EBW. The right panel (pressure) shows the coalescence of pressure waves some distance away from the EBW, and that a steady state detonation wave does not occur until about 1.5 microseconds after excitation begins. This acceleration of the initiation has been seen in LLNL experiments.

Ultimately, some distance away from the EBW, a steady state detonation of the PETN occurs, and initiation occurs as quickly as possible. If one were to trace back from this outer region inward to the instant in time when a prompt initiation of the powder would have had to occur at the EBW-PETN interface (found by tracing the steady state slope back toward zero radius – approximately 1 microsecond in this example), this instant is delayed relative to the burst time (which should be about 750 ns in the example, but is premature due to neglect of latent heats). This 250 ns of time is the so-called "EBW lost time" or "excess transit time" that is often referred to in classic EBW texts.[3,4] It represents the increased amount of time this gradual acceleration of initiation requires relative to what would be needed for prompt initiation at the EBW-powder interface.

Figure 4 summarizes the concept of the EBW lost time in diagrams. If an EBW-powder system is overdriven – that is, the shocks from the EBW are stronger and faster than steady state powder detonation – prompt initiation is expected and there is no lost time. When under-driven, the need for multiple shocks to coalesce to initiate the powder arises. As excitation decreases, this requires more space (resulting in apparent initiation further away from the EBW) and more time (the EBW lost time). At sub-threshold excitations, the shocks die out before they can effectively coalesce and initiate the powder.

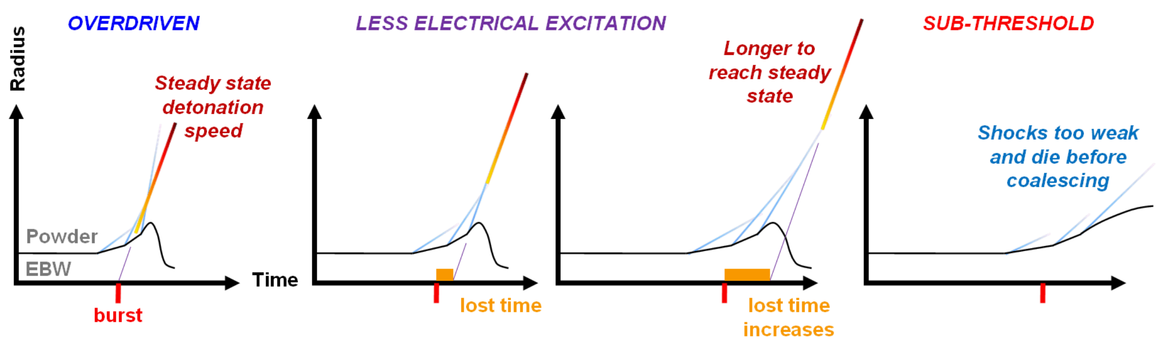

Figure 4. Basic explanation for EBW "lost time." When the system is overdriven (left) the shocks into the HE are faster than the steady state detonation speed of the powder, and there is essentially no time "lost" between burst and powder detonation. As excitation decreases, the dynamic processes of EBW burst slow down, and it takes more time (and more distance) for the EBW shocks to combine and become strong enough to light the powder (away from the EBW). This manifests itself as "lost time" due to delayed onset of steady state detonation. At sub-threshold excitations (right), the shocks die before they can combine to be strong enough to light the powder.

While significant room for improvement exists, and will be pursued, these simple EBW models suggest a basic framework for how EBW-mode powder initiation occurs in common EBW detonators. Meanwhile, EBW models have been generalized to more complicated geometries for a variety of different sensitivity studies.

EBF & Slapper Modeling Methods & Results

No practical EBW detonator system is actually 1-D. Header effects are inherently 2-D and once end effects are considered, the full system is inherently 3-D. To capture some of these effects, 2-D models have been created in CALE, and both 2-D and 3-D models have been created in another MHD-capable LLNL-developed hydrodynamic code, ALE3D.

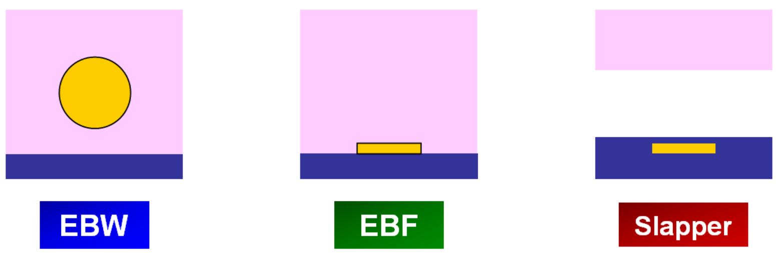

Figure 5. Modeling representations of different initiator types. An EBF used "in an EBW mode" is in intimate contact with the powder, but initiates the powder in the same way as an EBW – the rapid expansion of the bridge as it bursts sends initiating shocks into the surrounding low-density first-stage HE. By contrast, a slapper is an EBF that is over-coated with a flyer material. As the slapper's EBF bursts, it accelerates the flyer over a gap until it impacts a higher-density first-stage pellet.

Figure 5 shows the basic geometric differences between EBWs, EBFs and slappers. In all three cases, the initiator dynamics are similar (as described above for EBWs), and the resulting electrical waveforms are similar. Slappers are inherently different, however, in that typically, a higher density pellet is used, and an inert layer of material, the flyer, is accelerated by the expanding initiator plasma until it impacts the pellet. In this case, initiation is truly an impact initiation, and multiple established methods exist to model the impact initiation of the pellet (so modeling of the impact initiation is somewhat unnecessary here). In some cases where flyer barrels are small in diameter, and fly-distances are small, the expansion of the plasma does take some part in initiating the pellet also, and the full model is needed. Otherwise, the problem could be split into two decoupled parts: flyer generation and impact initiation of the pellet.

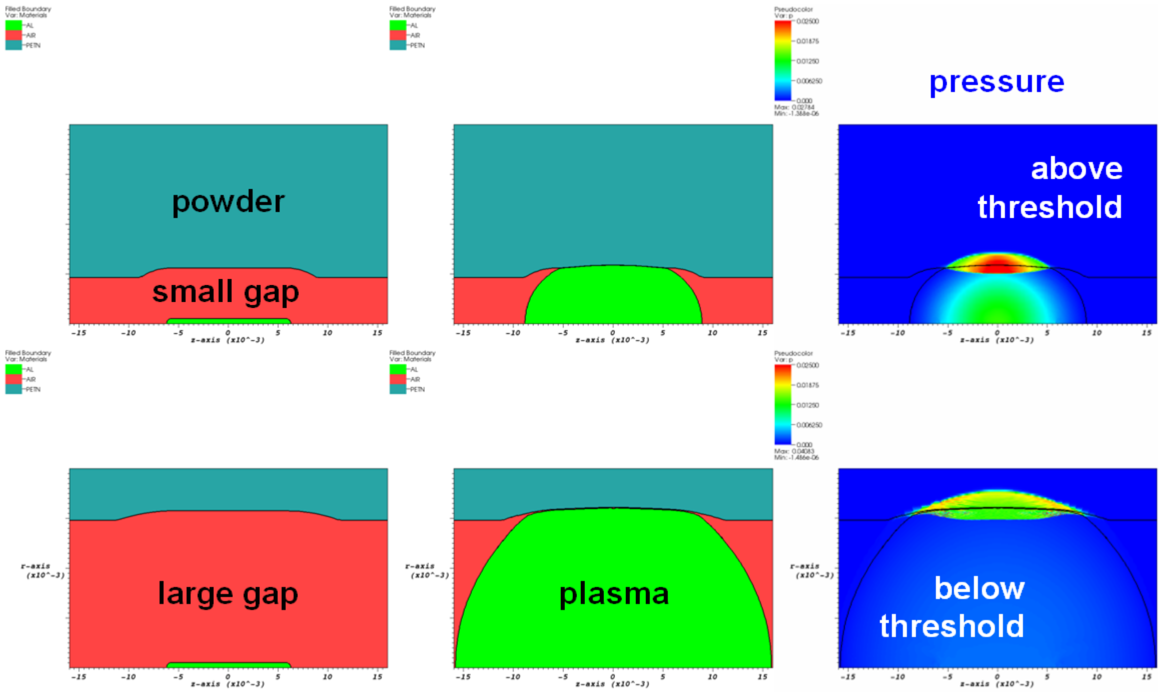

Figure 6. Modeling the sensitivity of an EBF design to gaps between the bridge and the powder. Far right panels show pressure (on the same scale) as opposed to materials (middle and left). The top series shows a small gap model and how the pressure imparted to the powder is still sufficiently large to cause initiation. By contrast, the bottom series shows a large gap model in which the powder does not initiate.

Figure 6 shows a 2-D CALE EBF model that considers the possibility of gap formation between the powder and the EBF. Such hypothetical gap formation is the potential result of sintering that may occur as a PETN powder ages. EBF designs can be sensitive to this type of gap formation because the plasma must expand somewhat before the powder is even shocked. This delay robs the powder of some of the excitation it would have received if the plasma did not expand freely into the gap. Such models are useful for evaluating the sensitivity of a design to this type of aging phenomenon, and for predicting how much of a gap can be tolerated before detonator performance is impaired.

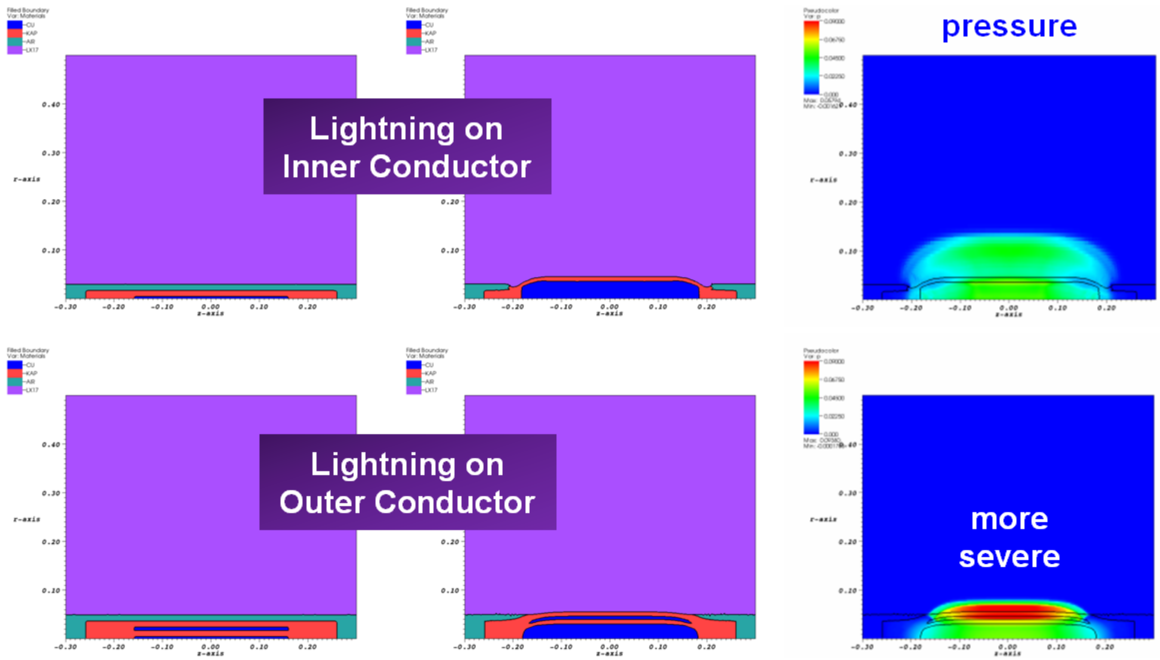

Figure 7. Modeling lightning strike scenarios. Assuming a stand-off between shielded conductors and the HE charge they run against, the conductors when exploded by extreme currents (lightning) are hypothesized to initiate the charge (although the excitation to the HE has been shown to be quite small). The top series shows the scenario if lightning is on the inner conductor (in a 2-conductor system), whereas the bottom series shows that excitation of the outer conductor uses the inner conductor as increased slapper mass, and is thus more severe.

Another scenario that is considered is the possibility of extremely large excitations on large ribbon conductors that run along side HE charges, the so-called "lightning strike" scenario. In this scenario, the lightning effectively turns the shielded conductor into a slapper, the dielectric jacket of the conductor serving as a flyer. Note that for the conductor-slapper to be effective, a sufficient standoff must also exist between the conductor and the charge. The scenario is admittedly hard to achieve in the first place, and furthermore, preliminary modeling, introduced in **Figure 7**, appears to be predicting that initiation of high-density insensitive high explosives (IHEs) such as LX-17 or PBX 9502 is extremely unlikely, given the scenario. This work is still in progress and requires more simulations and validation to be considered complete.

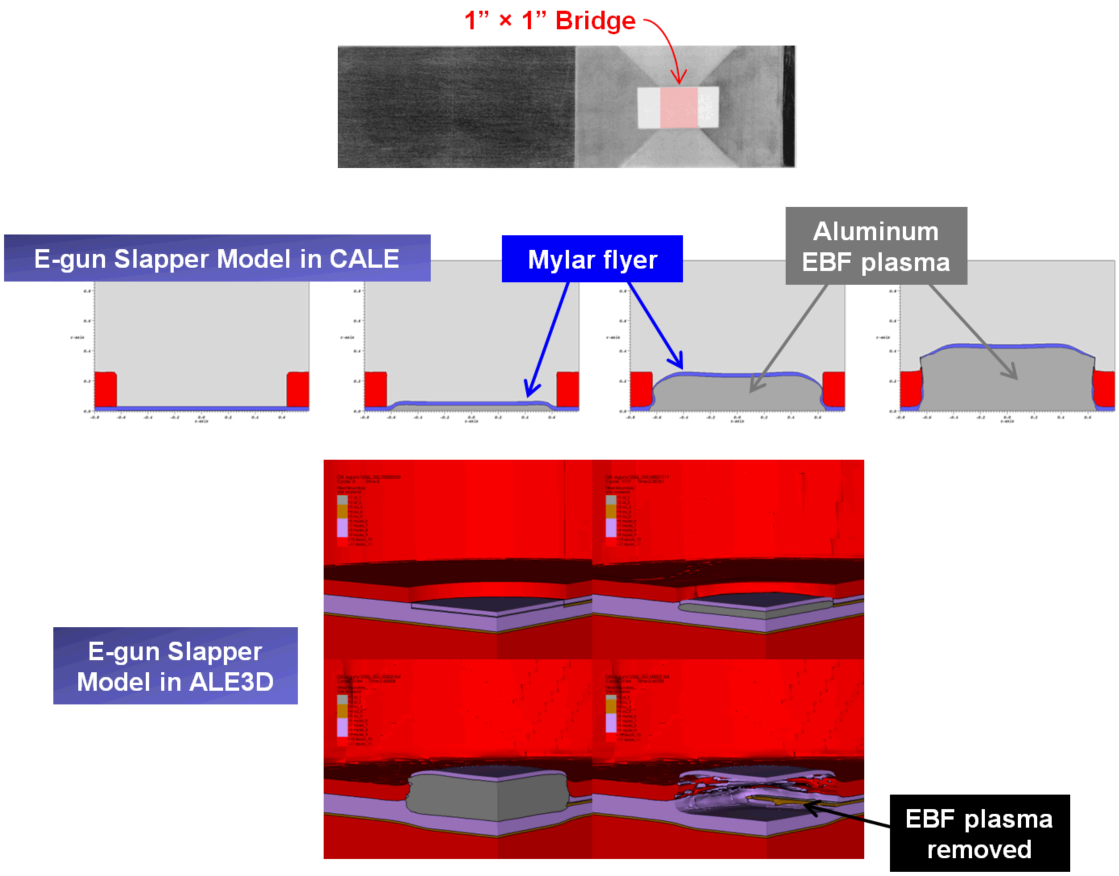

Figure 8. E-gun slapper models. The E-gun throws a very large flyer as a simulation of the lightning strike scenario. These simulations show general agreement between the 2-D code CALE and the 3-D code ALE3D in predicting flyer shapes. Comparison of flyer speeds and electrical waveforms with experimental data is currently under way.

An experimental approximation of the lightning strike scenario exists in electric gun (or “E-gun”) experiments. The LLNL E-gun is a large capacitor (up to 40 KV and 45 KJ), capable of launching 1-inch (25.4 mm) diameter flyers into an explosive. A typical E-gun slapper is shown in **Figure 8**, along with 2-D CALE and 3-D ALE3D simulations of the slapper. The E-gun slapper experiment provides a rich data set that we can validate our simulations against, providing some confidence that extrapolations out to the more far-fetched lightning strike regime are believable.

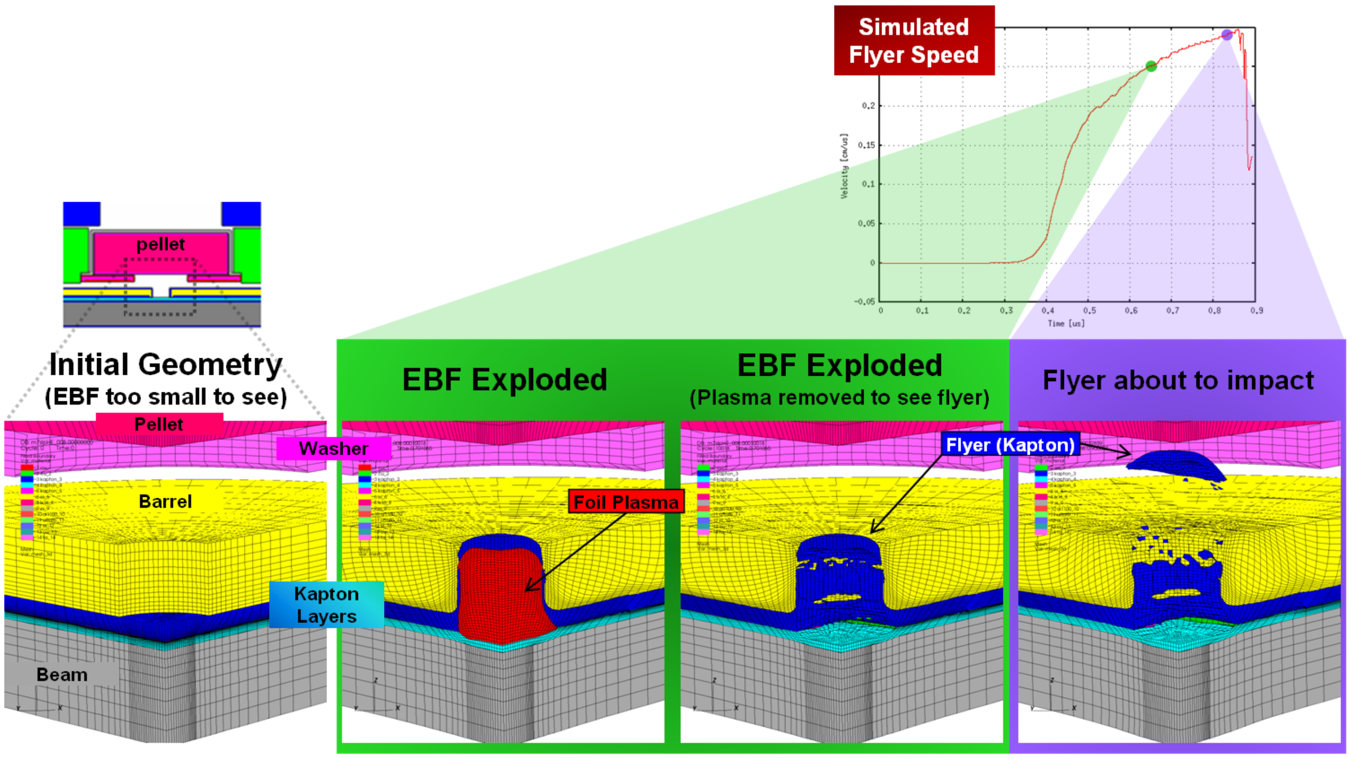

Figure 9. Slapper detonator modeling. This series shows the evolution of a flyer from a typical slapper detonator design. Studies to validate the predicted flyer speed, shape and impact pressure are planned.

The final example shown here in **Figure 9** is our preliminary model of a typical mid-size slapper detonator, where a Kapton flyer is launched into a high-density PETN-based pellet. The ultimate goal is to make changes in a validated model that would represent hypothetical aged configurations, and predict the sensitivity of performance upon them, thus creating a slapper detonator lifetime model. Other current work in the simulation of very small "chip-slapper" detonators is also under way, including sensitivity studies useful in guiding active design modifications.

Fully-coupled MHD initiator simulations using finite element codes such as these are still fairly new at LLNL, and gaining more interest and potential applications. The insight provided from even the simplest of models appears valuable, as well as predictions from more specifically tailored analyses.

Acknowledgments

The authors wish to thank Jeffrey D. Hagerty, Ronald S. Lee and Chadd M. May, leaders of the Initiation Systems Group, Initiation Physics Group and Detonation Science Project (respectively) at LLNL. Thanks for support from Ronald Streit and William Mclean of the Nuclear Safety R&D Program and Enhanced Surveillance Campaign (respectively). Thanks also to Robert Tipton, Wes Davis, Wigbert Siekhaus, Paul Wilkins, James McCarrick and David Steich for multiple valuable conversations and peer review.

This work was performed under the auspices of the U.S. Department of Energy by Lawrence Livermore National Laboratory under contract DE-AC52-07NA27344.

References

[1] Hrousis, C.A. "Modeling Initiation in Exploding Bridgewire Detonators." *36th Annual Meeting of ICT combined with 32nd International Pyrotechnics Seminar,* 2005, Karlsruhe, Germany, section V42.

[2] Tarver, C.M., Halquist, J.O. and Erickson, L.M. "Modeling Short Pulse Duration Shock Initiation of Solid Explosives." *8th International Detonation Symposium,* 1985, Albuquerque, NM, p. 951.

[3] Chace, W.G. and Moore, H.K. *Exploding Wires.* Plenum Press, Inc. New York. 1959.

[4] Cooper, P.W. *Explosives Engineering.* Wiley-VCH, Inc. New York. 1996. p. 365.